A Novel Approach for Experimental Measurement of Scatter Profile and Scatter to Primary Ratio in 64-Slice CT Scanner

A. Akbarzadeh[1], M.R. Ay[1,2] , H. Ghadiri[2,3], S. Sarkar[1,2] and H. Zaidi[4]

[1] Department of Medical Physics and Biomedical Engineering, School of Medicine, Medical Sciences/ University of Tehran, Tehran, Iran
[2] Research Center for Science and Technology in Medicine, Medical Sciences/ University of Tehran, Tehran, Iran
[3] Department of Medical Physics, Iran University of Medical Sciences, Tehran, Iran
[4]Division of Nuclear Medicine, Geneva University Hospital, CH-1211 Geneva, Switzerland

Abstract— **scattered radiation is an important source of artifacts in x-ray CT imaging and its detrimental effects have become much stronger in 64-slice CT scanners with extended detector aperture. The magnitude and spatial distribution of the scatter component should be corrected for before or during the reconstruction process. Thorough knowledge of scatter distribution is essential for development of scatter correction algorithms. In this study a novel approach based on using dedicated blockers is proposed to efficiently calculate scatter profiles and scatter to primary ratio (SPR) in different detector rows in a CT scanner with 64-slice capability. The influence of different parameters such as tube voltage, phantom size and phantom off-centering on the scatter profile and SPR was quantitatively measured based on the developed method. The SPR decreases from 219.9 to 39.9 when the tube voltage increases from 80 kVp to 140 kVp in 21.5 cm water phantom. The proposed method is easy to use and straightforward and can be used for any measurement.**

Keywords— **Scatter, SPR, CT, Tube Voltage**

I. Introduction

There are several sources of error and artefact that affect clinical image quality in x-ray computed tomography (CT). It is therefore essential to assess their significance and effect on the resulting images to reduce their impact either by optimizing the scanner design or by devising appropriate image correction and reconstruction algorithms. One of the most important parameters in x-ray CT imaging is the noise induced by detected scattered radiation, which depends on the geometry of the CT scanner and the object under study [1, 2].

It is well established that contamination of CT data with scattered radiation reduces reconstructed CT numbers and introduces cupping artefacts in the reconstructed images. This effect is more pronounced in multi detector CT scanners with extended detector aperture mostly using cone-beam configurations, which are much less immune to scatter than fan-beam and single-slice CT scanners. The magnitude and spatial distribution of scattered radiation in x-ray CT should be accurately quantified for optimization of scanner design geometry and development of robust scatter correction techniques. This problem has been historically addressed by different groups in the context of using CT for quantitative measurements using experimental studies, mathematical modelling and Monte Carlo simulations for both fan- and cone-beam geometries. It should be noted that most published papers assessing the distribution of scattered radiation in the fan-beam geometry used either simple experimental measurements relying on single blockers [3,4, 5] or comprehensive Monte Carlo simulations [6, 7, 8].

In this work, we propose a new method based on using dedicated blockers for accurate measurement of scatter profile and scatter to primary ratio (SPR) in all detector rows in a CT scanner with 64-slice capability. The method can in principle be used for any scanner geometry and configuration. In contrast to previously published methods for measuring scattered radiation (limited to one measurement point), the proposed method measures scattered radiation in almost all detector channels.

II. Materials and Methods

A. Acquisition System

The 64 slice Light Speed VCT scanner (GE Healthcare Technologies, Waukesha, WI) with Highlight ($Y_2Gd_2O_3$:Eu) ceramic scintillators was used in this work. This third generation CT scanner has 540 mm source to isocenter and 950 mm source to detector distance, 58,368 individual elements arranged in 64 rows of 0.625 mm thickness at isocenter, each containing 888 active patient elements and 24 reference elements. The scanner is equipped with the Performix Pro Anode Grounded Metal-Ceramic Tube Unit which uses 56 degree fan angle, 7 degree target angle and minimum inherent filtration of 3.25 mm Al and 0.1 mm Cu at 140 kVp.

B. Phantoms

Two physical phantoms were constructed to measure the scattered radiation profile and SPR., namely a water cylindrical phantom with 215 mm internal diameter and 6 mm Plexiglas wall thickness and a uniform Polypropylene cylindrical phantom with 300 mm diameter.

N.A. Abu Osman, F. Ibrahim, W.A.B. Wan Abas, H.S. Abd Rahman, H.N. Ting (Eds.): Biomed 2008, Proceedings 21, pp. 473–477, 2008
www.springerlink.com

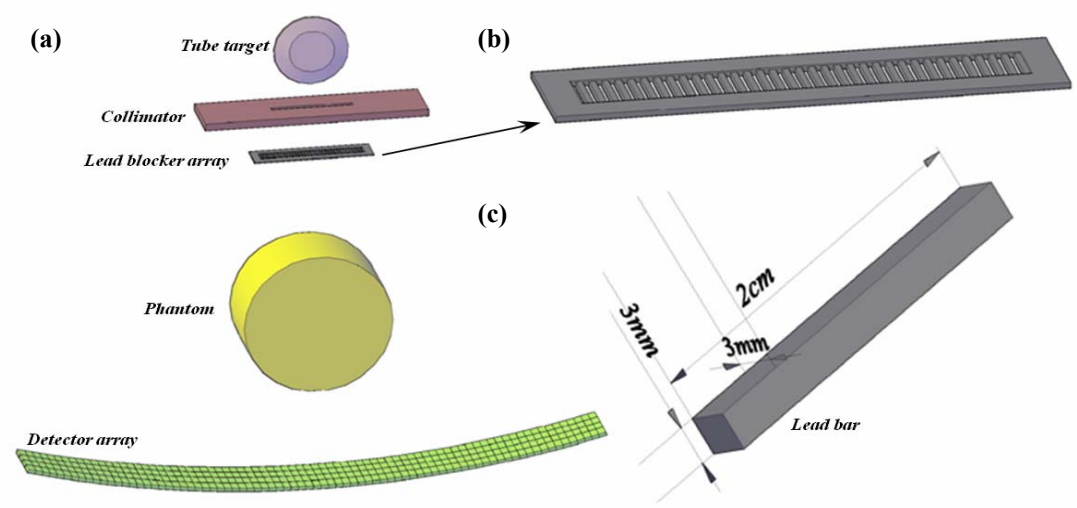

Fig 1: (a) Schematic drawing of setup utilized for scatter profile estimation. (b) Lead blocker array. (c) Lead bar and its dimensions.

C. *Lead blocker array*

The experimental measurement of SPR involves the use of a small lead blocker. In this method, the blocker is placed on top of the phantom where the x-ray intensity behind the phantom and under the lead blocker indicates the amount of scattered radiation. The main limitation of this method is that it only allows calculation of the SPR in one point. In this study instead of using a small blocker, we have used a lead blocker array consisting of 20 lead bars with 3 mm thickness that is placed after the collimator (Fig. 1a). After irradiating the phantom in presence of the lead blocker array, it is possible to measure the scattered and primary radiation in several detector channels. This method offers the possibility of calculating the scattered and primary radiation and also SPR in several points using just one irradiation. Figure 1 shows the experimental setup and geometry of the lead blocker array.

D. *Methods*

In order to calculate scatter profiles (the amount of scattered radiation in several detector channels), the lead blocker array was inserted between the collimator and the phantom during x-ray tube exposure with different tube voltage (kVp) and current (mA) settings. Since the lead blocker array itself is another source of scatter, exposure is repeated without the phantom in the field of view to enable measurement of the lead blocker array's scatter and eliminate it from the scatter profile. It should be noted that all measurements in this study were carried out without the bow-tie filter which is normally placed into the collimator box.

In the next step, the detector read-out (CT raw data file from the scanner database) was transferred to a host PC for off-line processing. The 16 digit binary file contains the whole 912×64 detector readings of the 64 detector rows with 912 detector channels in each row. The Light Speed VCT scanner's Data Acquisition System hardware uses some calibration factors to reduce high values of detector readings to 16 digit range thus enabling to compress data size. Whenever scanner software performs reconstruction and correction procedures, these calibration factors must be applied inversely to get the real data following file reading.

To compute the real values, a computer program was developed under Matlab 7.4 (The MathWorks Inc., Natick, MA, USA) which reads the binary file and generates a two-dimensional matrix (912×64) as output. As this matrix is supposed to reflect real read-out of detectors, the above mentioned calibration factors were applied inversely on the output matrix.

The final 64×912 calibration matrix was divided into two areas: (1) shadowed area whose detector channels were exactly within the shadow of lead bars in the blocker array. (2) exposed area whose detector channels were exposed and recorded both scatter and primary (i.e. total) radiation. It was assumed that matrix elements assigned to the shadowed area contain essentially scattered radiation. A program running under Matlab 7.4 was developed in order to extract and separate these two areas. Scatter and total radiation profiles were obtained for all channels using interpolation. Primary radiation was computed by subtracting scattered radiation from total radiation. SPR estimates were calculated for all detector channels.

III. Results

A. Scatter profiles

Figure 2 shows the scatter profile calculated from detector row 32 (the central row) at different x-ray tube voltages and fixed tube current (100 mA). It should be noted that the cylindrical water phantom was irradiated for three seconds in this measurement.

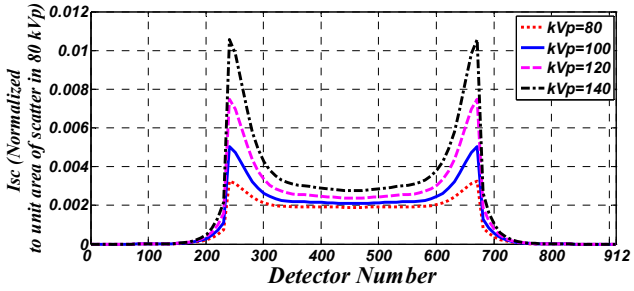

Fig 2: Scattered radiation profile for cylindrical water phantom, at different tube voltages and 100 mA tube current (3 seconds exposure).

Figure 3 shows the measured scatter profile at different tube voltages for the cylindrical Polypropylene phantom with 300 mm diameter irradiated for three seconds with 200 mA tube current.

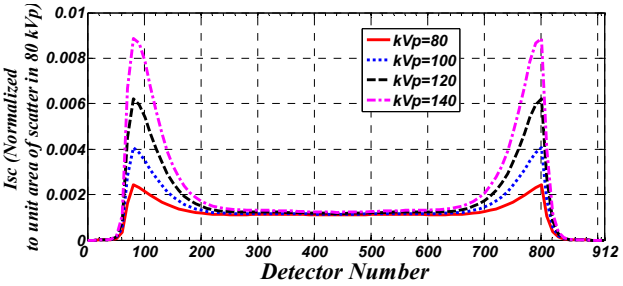

Fig 3: Scattered radiation profile for cylindrical Polypropylene phantom at different tube voltages and 200 mA tube current.

B. Scatter to primary ratio

The pollution of projection data with scattered photons was investigated qualitatively by calculation of the SPR as function of phantom size, phantom material, tube voltage and phantom off-centring as illustrated in figures 4-7. Figure 4 shows the calculated SPR for the cylindrical water phantom at different tube voltages and 100 mA current.

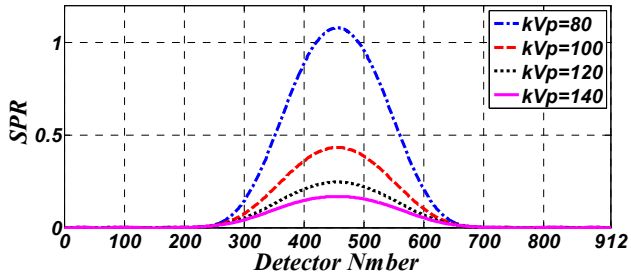

Fig 4: Calculated SPR profiles for the water phantom at different tube voltages and 100 mA tube current.

Figure 5 shows the calculated SPR for the Polypropylene phantom at different tube voltages and 200 mA current. The Polypropylene phantom was used in order to mimic clinical conditions for obese patients.

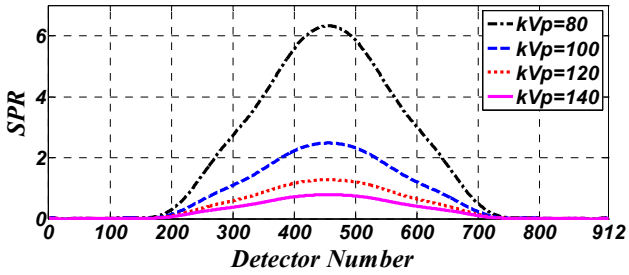

Fig 5: Calculated SPR profiles for Polypropylene phantom at diferent tube voltages and 200 mA tube current.

C. Integrated SPR

Figure 6 shows the integrated SPR (the sum of SPRs in each detector channel located in one row) for different detector rows when the water phantom is irradiated at different tube voltages.

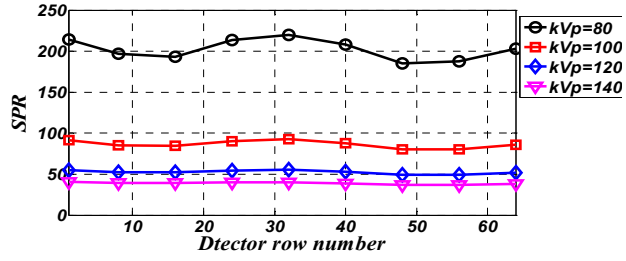

Fig 6: Integrated SPR for different detector rows in 64-slice CT scanner obtained for the water phantom iradiated at different tube voltages.

The integrated SPR values for detector row number 32 is 219.5, 92.5, 55.2, and 39.9 for tube voltages of 80, 100, 120 and 140 kVp, respectively.

N.A. Abu Osman, F. Ibrahim, W.A.B. Wan Abas, H.S. Abd Rahman, H.N. Ting (Eds.): Biomed 2008, Proceedings 21, pp. 473–477, 2008
www.springerlink.com

Figure 7 shows the integrated SPR for detector row 32 (central row) when the phantom is shifted several centimeters toward (positive value) and away from (negative value) the detector. This figure illustrates the variability of SPR with respect to the distance between the phantom and the detector. Generally, the SPR decreases with increasing the distance between the phantom and the detector.

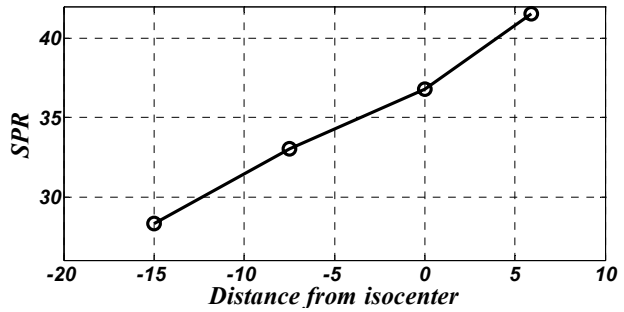

Fig 7: Integrated SPR in the water phantom calculated for different distances between the phantom and detectors (positive: toward the detector and negative: toward the x-ray tube) for tube current of 100mA and tube voltage 120kVp.

IV. Discussion

The experimental measurements performed using the lead blocker array proved that the method can be effectively be used for calculation of scattered radiation distribution and SPR given that the results obtained are in good agreement results reported in the literature.

The two peaks in the scatter profile observed in figures 2 and 3 are due to the trade-off between increasing the probability of Compton scattering while decreasing the transmission probability of scattered photons from the bow-tie filter with increasing the attenuation length. It should be emphasized that the lower scattered photons in the center of the profile covered by the phantom whose diameter is large compared to the mean free path of photons is the result of either absorption of incoming photons before undergoing a Compton event or attenuation of scattered photons after Compton scattering.

The higher SPR value in 80 kVp in figures 4 and 5 is due to the fact that transmitted primary radiation increases by increasing tube voltage. On the other hand, it is well known that the probability of compton scattering increases with increasing tube voltage (Figure 2 and 3). As a matter of fact, the amount of primary photons increases much more than the amount of scattered photons by increasing tube voltage. Therefore, the SPR decreases with increasing tube voltage.

It has been reported that increasing the distance between the phantom and detectors decreases the SPR estimates [1,5,6,8]. This effect has been known as air-gap effect. However, increasing distance between the phantom and detector causes reduction in scattered photons recorded by the detector.

V. Conclusion

In this study we presented a novel approach for measurement of scattered radiation distribution and SPR in a CT scanner with 64-slice capability using lead block array. The method can also be used on other multislice CT scanners. The proposed technique can accurately estimate scatter profiles. It is relatively straightforward, easy to use, and can be used for any related measurement. Accurate estimation of the magnitude and spatial distribution of scattered radiation using the proposed method can be used for optimization of scanner design geometry and development and optimization of robust scatter correction techniques which certainly is curtail for new generation of CT scanners with 256 [9] and 320 slice capability introduced commercially by the end of 2007.

Acknowledgment

This work was supported by Medical Sciences/University of Tehran, Tehran, Iran and the Swiss National Foundation under grant No. 3152A0-102143.

References

1. Tofts P S and Gore J C 1980 Some sources of artefact in computed tomography Phys. Med. Biol. 25 117–127
2. Johns P C and Yaffe M 1982 Scattered radiation in fan beam imaging systems Med. Phys. 9 231–9
3. Joseph P M and Spital R D 1982 The effects of scatter in x-ray computed tomography Med. Phys. 9 464–472
4. Glover G H 1982 Compton scatter effects in CT reconstructions Med. Phys. 9 860–7
5. Siewerdsen J H and Jaffray D A 2001 Cone-beam computed tomography with flat-panel imager: magnitude and effects of x-ray scatter Med. Phys. 28 220–231
6. Ay M R and Zaidi H. 2005 Development and validation of MCNP4C-based Monte Carlo simulator for fan- and cone-beam x-ray CT. Phys. Med. Biol. 50:4863-4885.
7. Colijn A P and Beekman F J 2004 Accelerated simulation of cone beam x-ray scatter projections IEEE Trans. Med.Imaging 23 584–590
8. Malusek A, Sandborg M P and Carlsson G A 2003 Simulation of scatter in cone beam CT: effects on projection image quality SPIE Medical Imaging 2003: Physics of Medical Imaging (San Diego, CA, USA) SPIE vol 5030; pp 740–751
9. Endo M., Mori S., Tsunoo T., Miyazaki H. 2006 Magnitude and effects of x-ray scatter in a 256-slice CT scanner Med. Phys. 33 3359–3368

Corresponding Author:

Author: Mohammad Reza Ay
Institute: School of Medicine, Medical Sciences/ University of Tehran
Street: Pour Sina
City: Tehran
Country: Iran
Email: mohammadreza_ay@tums.ac.ir

N.A. Abu Osman, F. Ibrahim, W.A.B. Wan Abas, H.S. Abd Rahman, H.N. Ting (Eds.): Biomed 2008, Proceedings 21, pp. 473–477, 2008